Improved effective vertices in the multiorbital two-particle self-consistent method from dynamical mean-field theory

Karim Zantout,[1] Steffen Backes,[2,3,4] Aleksandar Razpopov,[1] Dominik Lessnich,[1] and Roser Valentí[1]

[1]*Institute for Theoretical Physics, Goethe University Frankfurt, Max-von-Laue-Strasse 1, 60438 Frankfurt am Main, Germany*

[2]*Research Center for Advanced Science and Technology, University of Tokyo, Komaba, Tokyo 153-8904, Japan*

[3]*Center for Emergent Matter Science, RIKEN, Wako, Saitama 351-0198, Japan*

[4]*CPHT, CNRS, École polytechnique, Institut Polytechnique de Paris, 91128 Palaiseau, France*

(Received 22 November 2022; revised 3 April 2023; accepted 23 May 2023; published 1 June 2023)

In this paper, we present a multiorbital form of the two-particle self-consistent approach (TPSC) where the effective local and static irreducible interaction vertices are determined by means of the dynamical mean-field theory (DMFT). This approach replaces the approximate ansatz equations for the double-occupations $\langle n_{\alpha,\sigma} n_{\beta,\sigma'} \rangle$ by sampling them directly for the same model using DMFT. Compared to the usual Hartree-Fock-like ansatz, this leads to more accurate local vertices in the weakly correlated regime and provides access to stronger correlated systems that were previously out of reach. This approach is extended by replacing the local component of the TPSC self-energy by the DMFT impurity self-energy, which results in an improved self-energy that incorporates strong local correlations but retains a nontrivial momentum dependence. We find that this combination of TPSC and DMFT provides a significant improvement over the multiorbital formulation of TPSC as it allows to determine the components of the spin vertex without artificial symmetry assumptions and opens the possibility to include the transversal particle-hole channel. The new approach is also able to remove unphysical divergences in the charge vertices in TPSC. We find a general trend that lower temperatures can be accessed in the calculation. Benchmarking single-particle quantities, such as the local spectral function with other many-body methods, we find significant improvement in the more strongly correlated regime.

DOI: 10.1103/PhysRevB.107.235101

I. INTRODUCTION

The study of correlated electron physics in solid-state systems poses many difficulties, of which the solutions are expected to be key ingredients for understanding emergent phenomena, such as unconventional superconductivity [1–10] or spin liquid phases [11–17]. As solving the many-electron problem exactly is impossible due to the large number of particles, effective low-energy lattice models have been developed, such as the Hubbard model, to describe the physics of correlated electrons in partially filled orbitals [18–20]. Even though this model is a significant simplification of the original problem, in general, an exact solution is not available, which led to the development of a large variety of approximate many-body methods for the Hubbard model [21–24]. Among the different approaches we focus here on the dynamical mean-field theory (DMFT) [25–27] and the two-particle self-consistent (TPSC) method [28–30].

The idea of DMFT is to map the original lattice problem onto an effective local model, embedded in an effective environment that is determined self-consistently. This approach restricts correlation effects to purely local but dynamical contributions and, thus, results in a momentum-independent but frequency-dependent self-energy $\Sigma(\omega)$. This approximation becomes exact in the limit of infinite coordination number, but it has been applied to great success in finite-dimensional strongly correlated electron systems [27,31–35]. On the other hand, DMFT cannot describe nonlocal correlation effects, which are relevant, e.g., in low-dimensional systems and the description of pseudogaps in the context of high-temperature cuprate superconductors [36–39]. Nonlocal extensions to DMFT that reintroduce a momentum dependence to the self-energy have been and are actively developed, such as cluster extensions [27,40–45] or different types of diagrammatic extensions, such as GW+DMFT [46–51], dynamical vertex approximation [21,52–54], TRILEX [55–57], QUADRILEX [58], D-TRILEX [59–62], dual fermion [63–65], and dual boson techniques [66–69]. Most of them come at a significant increase in computational cost, especially when multiorbital systems are considered.

Another way to access nonlocal and dynamical correlation effects is given by the TPSC approach [29,70]. Within TPSC, the two-particle irreducible vertex Γ, which contains information on two-particle scattering processes, is approximated to be an effective local and static quantity [70]. This effective interaction vertex Γ is determined by requiring the resulting spin and charge susceptibilities to fulfill corresponding local sum rules. The quasiparticle renormalization effects from spin and charge fluctuations eventually lead to a nonlocal and dynamical self-energy $\Sigma(k, \omega)$. In the case of weak- to intermediate-coupling strengths, TPSC has proven to yield accurate results [29,70], and it can be extended to multisite [71–76] and multiorbital [30,77,78] systems. The multiorbital TPSC formalism allowed for the investigation of possible spin-fluctuation pairing scenarios in unconventional superconductors [77] and nonocal correlation effects in the spectral properties of Fe-based superconductors [78,79] but still faces certain limitations, which we aim to address in this article.

One of the limitations of the multiorbital TPSC scheme is the occurrence of diverging negative charge vertices when one

requires the corresponding sum rules to be satisfied exactly, leading to unphysical negative spectral weight [30]. This issue can be circumvented by restricting the charge vertex search to non-negative values [30,77,78], at the expense of violating the corresponding local sum rules. Moreover, the usual ansatz equations do not allow for a determination of all double-occupations and correspondingly do not provide enough sum rules to determine all relevant elements of the spin vertex. Symmetry relations that hold for the bare spin vertex can be used to determine these elements but still pose an additional approximation and do not allow for a straightforward inclusion of the transversal particle-hole channel [30].

In this paper, we demonstrate that these limitations can be resolved by replacing the ansatz equations for the double-occupations with the double-occupations directly obtained from a DMFT calculation. This leads to effective local spin and charge vertices, which are consistent with the double-occupations obtained by DMFT and do not rely on the additional Hartree-Fock-like decoupling employed in the original ansatz equations. Our results show that this approach that we call $\langle nn\rangle_{\mathrm{DMFT}}$-TPSC, is able to improve or completely resolve the shortcomings of the original formulation of multiorbital TPSC. The idea of using the double-occupation as external parameter was already proposed in the original TPSC formulation [28]. In an additional step, the local self-energy of $\langle nn\rangle_{\mathrm{DMFT}}$-TPSC can be replaced by the impurity self-energy of DMFT, which we name $\langle nn\rangle_{\mathrm{DMFT}}$-TPSC+$\Sigma_{\mathrm{DMFT}}$. This replacement is motivated by the nonperturbative nature of the DMFT approximation, which has shown to be able to obtain accurate results for local quantities, such as the local self-energy and double-occupations [23,27,31]. The same extensions of TPSC but in the single-band case are presented in Ref. [80]. The article is structured as follows. In Sec. II, we present the multiorbital TPSC formalism from Ref. [30], discuss the limitations and motivate the combination with DMFT. In order to test our new approach, we perform calculations on a simple two-orbital Hubbard square lattice model as in Ref. [30]. In Sec. III, the results of this benchmark are presented and discussed, and Sec. IV contains a summary and addresses open questions.

II. MODEL AND METHOD

In this paper, we consider the fermionic multiorbital Hubbard-model, defined by the Hamiltonian,

$$\begin{aligned} H = &\sum_{\alpha,\beta,i,j,\sigma} \left(t_{\alpha\beta}^{\vec{R}_i-\vec{R}_j} - \mu\delta_{i,j}\delta_{\alpha,\beta}\right) c^{\dagger}_{\alpha,\sigma}(\vec{R}_i)c_{\beta,\sigma}(\vec{R}_j) \\ &+ \frac{1}{2}\sum_{\alpha,\beta,i,\sigma} U_{\alpha\beta} n_{\alpha,\sigma}(\vec{R}_i) n_{\beta,-\sigma}(\vec{R}_i) \\ &+ \frac{1}{2}\sum_{\substack{\alpha,\beta,i,\sigma \\ \alpha\neq\beta}} (U_{\alpha\beta} - J_{\alpha\beta}) n_{\alpha,\sigma}(\vec{R}_i) n_{\beta,\sigma}(\vec{R}_i) \\ &- \frac{1}{2}\sum_{\substack{\alpha,\beta,i,\sigma \\ \alpha\neq\beta}} J_{\alpha\beta}[c^{\dagger}_{\alpha,\sigma}(\vec{R}_i)c_{\alpha,-\sigma}(\vec{R}_i)c^{\dagger}_{\beta,-\sigma}(\vec{R}_i)c_{\beta,\sigma}(\vec{R}_i) \\ &+ c^{\dagger}_{\alpha,\sigma}(\vec{R}_i)c_{\beta,-\sigma}(\vec{R}_i)c^{\dagger}_{\alpha,-\sigma}(\vec{R}_i)c_{\beta,\sigma}(\vec{R}_i)], \end{aligned} \tag{1}$$

where $t_{\alpha\beta}^{\vec{R}_i-\vec{R}_j}$ are the hopping matrix elements between orbitals α and β that are connected by lattice vectors $\vec{R}_i - \vec{R}_j$. Here, we restrict ourselves to the paramagnetic phase. The Hubbard and Hund's coupling terms are denoted by $U_{\alpha\beta}$ and $J_{\alpha\beta}$, respectively. Throughout this paper we assume spherical symmetry with $U_{\alpha\alpha} = U$, and $U_{\alpha\beta} = U - 2J$ for $\alpha \neq \beta$. The operator $c_{\alpha,\sigma}(\vec{R}_i)$ destroys an electron with spin σ in the α orbital at unit-cell position $\vec{R}_i$, and $c^{\dagger}_{\beta,\sigma}(\vec{R}_j)$ creates an electron with spin σ in the β orbital at unit-cell position $\vec{R}_j$. The density operator is defined via $n_{\alpha,\sigma}(\vec{R}_i) := c^{\dagger}_{\alpha,\sigma}(\vec{R}_i)c_{\alpha,\sigma}(\vec{R}_i)$, and μ is the chemical potential.

In order to introduce the combined TPSC and DMFT approach to the multiorbital Hubbard model, we first start with a short summary of the single-orbital and multiorbital TPSC approach following Ref. [30].

A. Single-orbital TPSC

The two-particle self-consistent approach was originally developed for the single-band Hubbard model [29,70] based on an approximate expression for the Luttinger-Ward functional [81], namely, $\Phi[G] \approx G\Gamma G$, where G is the full Green's function and Γ is the two-particle irreducible vertex. Additionally, in TPSC, one approximates the irreducible vertex Γ to be local and time-independent quantity. The reasoning behind both approximations lies on the observation that, far away from phase transitions, higher-order correlation functions only contribute through their averages, which are assumed to be absorbed in an effective interaction vertex Γ. In TPSC, this effective interaction vertex Γ appears as effective constant spin and charge vertices Γ^{sp} and Γ^{ch}, respectively.

In order to determine the values of the effective vertices Γ^{sp} and Γ^{ch}, TPSC relies on the enforcement of the local spin and local charge sum rules,

$$\chi^{\mathrm{sp}}(\vec{R}=0,\tau=0) = \langle n\rangle - 2\langle n_{\uparrow}n_{\downarrow}\rangle, \tag{2}$$

$$\chi^{\mathrm{ch}}(\vec{R}=0,\tau=0) = \langle n\rangle + 2\langle n_{\uparrow}n_{\downarrow}\rangle - \langle n\rangle^2, \tag{3}$$

where $\chi^{\mathrm{sp/ch}}$ is the spin/charge susceptibility, τ denotes imaginary time, and n is the particle number operator. Although the susceptibilities $\chi^{\mathrm{sp/ch}}$ are obtained from a Bethe-Salpeter equation from the spin and charge vertices $\Gamma^{\mathrm{sp/ch}}$ and the bare susceptibility $\chi^0 = G^0 \star G^0$ (and the noninteracting Green's function G^0), the double-occupation $\langle n_{\uparrow}n_{\downarrow}\rangle$ entering Eqs. (2) and (3) is *a priori* unknown. In the multiorbital TPSC approach relate the spin vertex Γ^{sp} to the double-occupation $\langle n_{\uparrow}n_{\downarrow}\rangle$ by means of the ansatz,

$$\Gamma^{\mathrm{sp}} = U\frac{\langle n_{\uparrow}n_{\downarrow}\rangle}{\langle n_{\uparrow}\rangle\langle n_{\downarrow}\rangle}, \tag{4}$$

which corresponds to a Hartree-Fock-like decoupling as motivated in Ref. [82]. This relation is used to solve the local spin sum rule [Eq. (2)] for the double-occupation. This ansatz allows for a fully self-contained TPSC formulation, and it was demonstrated that the self-consistently determined double-occupations are in good agreement with quantum Monte Carlo results at temperatures above the renormalized classical regime. Although, for lower temperatures in the moderately

correlated regime, this ansatz was found to significantly underestimate the double-occupations [70,83–85].

Another option is to consider the double-occupation as an external parameter, which can be obtained by other many-body methods with higher precision, such as DMFT, which is one of the main goals of this article.

B. Multiorbital TPSC

Following the same line of arguments as in the single-orbital TPSC approach, one can extend the formalism to multiorbital Hubbard models. A detailed derivation and discussion can be found in Ref. [30]. Here, we focus on the main equations to motivate the idea of combining TPSC with DMFT.

The Bethe-Salpeter equation evaluates to the following expressions for the spin and charge susceptibilities:

$$\chi^{\mathrm{sp/ch}}(q, iq_n) = 2[1 \mp \chi^0(q, iq_n)\Gamma^{\mathrm{sp/ch}}]^{-1}\chi^0(q, iq_n), \quad (5)$$

where q is a reciprocal lattice vector, q_n is the nth bosonic Matsubara frequency, and $\chi^0 = G^0 \star G^0$ is the noninteracting irreducible susceptibility given as a convolution ($\star$) of two noninteraction Green's functions G^0. The Hartree-Fock-like decoupling, which leads to Eq. (4) can be also applied to the multiorbital case [86], which results in

$$\begin{aligned} \Gamma^{\mathrm{sp}}_{\alpha\alpha\alpha\alpha} &= A^{\sigma}_{\alpha}, \\ \Gamma^{\mathrm{sp}}_{\alpha\alpha\beta\beta} &= B^{\uparrow,\downarrow}_{\alpha\beta} - B^{\downarrow,\downarrow}_{\alpha\beta}, \end{aligned} \quad (6)$$

where

$$A^{\sigma}_{\alpha} = U_{\alpha\alpha}\frac{\langle n_{\alpha\sigma}n_{\alpha,-\sigma}\rangle}{\langle n_{\alpha,\sigma}\rangle\langle n_{\alpha,-\sigma}\rangle}, \quad (7)$$

$$B^{\sigma,\sigma}_{\alpha\beta} = (U_{\alpha\beta} - J_{\alpha\beta})\frac{\langle n_{\alpha,\sigma}n_{\beta,\sigma}\rangle}{\langle n_{\alpha,\sigma}\rangle\langle n_{\beta,\sigma}\rangle}, \qquad \alpha \neq \beta, \quad (8)$$

$$B^{\sigma,-\sigma}_{\alpha\beta} = U_{\alpha\beta}\frac{\langle n_{\alpha,\sigma}n_{\beta,-\sigma}\rangle}{\langle n_{\alpha,\sigma}\rangle\langle n_{\beta,-\sigma}\rangle}, \qquad \alpha \neq \beta. \quad (9)$$

These ansatz equations provide no expression to determine the spin-vertex elements for the orbital combinations $\alpha\beta\alpha\beta$ and $\alpha\beta\beta\alpha$. A possible solution is to assume a symmetric form of the spin vertex, namely,

$$\Gamma^{\mathrm{sp}}_{\alpha\beta\beta\alpha} = \Gamma^{\mathrm{sp}}_{\alpha\beta\alpha\beta} = \Gamma^{\mathrm{sp}}_{\alpha\alpha\beta\beta}, \quad (10)$$

that is motivated from the bare $\Gamma^{\mathrm{sp},0}$, which obeys this symmetry in the longitudinal particle-hole channel [30]. The bare and dressed spin/charge vertices then enter the multiorbital TPSC self-energy expression [30],

$$\Sigma_{\alpha\delta,\sigma} = [\Gamma^{\mathrm{ch}}\chi^{ch}\Gamma^{\mathrm{ch},0} + \Gamma^{\mathrm{sp}}\chi^{sp}\Gamma^{\mathrm{sp},0}]_{\delta\bar{\beta}\alpha\bar{\gamma}} \star G^0_{\bar{\gamma}\bar{\beta}}. \quad (11)$$

The ansatz equations (6) and (10) together with the local spin and charge sum rules for the orbital index combinations for $\alpha\alpha\alpha\alpha$, $\alpha\alpha\beta\beta$, and $\alpha\beta\alpha\beta$ form a system of determined equations that can be solved to obtain the elements of the effective spin/charge vertices.

The shortcomings of the ansatz equations for the double-occupation observed in the single-orbital case become visible when approaching the renormalized classical regime or at large interaction strength [70]. These also seem to transfer to the multiorbital case where a qualitatively different behavior as a function of interaction strength was found for the equal-spin double-occupation $\langle n_{\alpha,\sigma}n_{\beta,\sigma}\rangle$ in TPSC compared to DMFT [30]. Furthermore, the TPSC double-occupations can result in negative diverging charge vertices $\Gamma^{\mathrm{ch}}_{\alpha\alpha\beta\beta}$, leading to unphysical negative spectral weight. These unphysical solutions can be avoided by restricting the charge vertex $\Gamma^{\mathrm{ch}}_{\alpha\alpha\beta\beta}$ to non-negative values, at the cost of violating the corresponding local charge sum rules [30].

These shortcomings of the ansatz equations for the double-occupations pose a significant limitation of the multiorbital formulation of TPSC especially in the moderately to stronger correlated regime. In the following, we will show how these limitations can be overcome by the combination of DMFT-derived double-occupations with TPSC, which we refer to as $\langle nn\rangle_{\mathrm{DMFT}}$-TPSC.

C. $\langle nn\rangle_{\mathrm{DMFT}}$-TPSC

In the multiorbital formulation of TPSC, there are not enough ansatz equations to determine the elements $\Gamma^{sp}_{\alpha\beta\alpha\beta}$ and $\Gamma^{sp}_{\alpha\beta\beta\alpha}$ and double-occupations self-consistently without further assumptions or approximations. For this reason, we propose to use the double-occupations obtained from a different many-body method for the same model, such as DMFT. Together with the local spin and charge sum rules for the susceptibilities $\chi^{sp/ch}_{\alpha\alpha\alpha\alpha}$, $\chi^{sp/ch}_{\alpha\alpha\beta\beta}$, and $\chi^{sp/ch}_{\alpha\beta\alpha\beta}$ the corresponding vertex elements $\Gamma^{sp/ch}_{\alpha\alpha\alpha\alpha}$, $\Gamma^{sp/ch}_{\alpha\alpha\beta\beta}$, and $\Gamma^{sp/ch}_{\alpha\beta\alpha\beta}$ can be determined without the need for additional approximations or symmetry assumptions. Only for the remaining elements $\Gamma^{\mathrm{sp/ch}}_{\alpha\beta\beta\alpha}$ for which the sum rules do not result in density-density correlation terms, we retain the symmetry relation,

$$\Gamma^{\mathrm{sp/ch}}_{\alpha\beta\beta\alpha} = \Gamma^{\mathrm{sp/ch}}_{\alpha\beta\alpha\beta}. \quad (12)$$

Furthermore, this approach allows for restoring crossing symmetry in the multiorbital TPSC formalism [87] by averaging the self-energy expressions from the longitudinal and transversal particle-hole channel [29,85], which yields for the nonzero elements of the spin vertex,

$$\begin{aligned} \Gamma^{\mathrm{sp},0}_{\alpha\alpha\alpha\alpha} &= 3U_{\alpha\alpha}/2, \\ \Gamma^{\mathrm{sp},0}_{\alpha\alpha\beta\beta} &= 2J_{\alpha\beta} - U_{\alpha\beta}/2, \\ \Gamma^{\mathrm{sp},0}_{\alpha\beta\alpha\beta} &= J_{\alpha\beta}/2 + U_{\alpha\beta}, \\ \Gamma^{\mathrm{sp},0}_{\alpha\beta\beta\alpha} &= 3J_{\alpha\beta}/2, \end{aligned} \quad (13)$$

and charge vertex,

$$\begin{aligned} \Gamma^{\mathrm{ch},0}_{\alpha\alpha\alpha\alpha} &= U_{\alpha\alpha}/2, \\ \Gamma^{\mathrm{ch},0}_{\alpha\alpha\beta\beta} &= 3U_{\alpha\beta}/2 - J_{\alpha\beta}, \\ \Gamma^{\mathrm{ch},0}_{\alpha\beta\alpha\beta} &= \Gamma^{\mathrm{ch},0}_{\alpha\beta\beta\alpha} = J_{\alpha\beta}/2 \end{aligned} \quad (14)$$

for the vertices in the self-energy expression Eq. (11). This variant of the multiorbital formulation of TPSC that determines the effective charge and spin vertices consistent with

another many-body method we call $\langle nn\rangle_X$-TPSC, where X can, in principle, be any method that obtains accurate estimates of the double-occupations.

In this paper, we focus on double-occupations that are extracted from DMFT, which has been shown to obtain reliable estimates for local quantities as long as nonlocal correlations are not too strong [27,31].

D. $\langle nn\rangle_{\text{DMFT}}$-TPSC+$\Sigma_{\text{DMFT}}$

As an additional step, we propose a scheme where the impurity self-energy obtained from DMFT is combined with the nonlocal part of the TPSC self-energy, which can be seen as an approximation to a fully self-consistent TPSC+DMFT calculation. This scheme would correspond to a situation where the nonlocal correlation effects are relevant but not strong enough to have a significant feedback on the local correlation effects obtained within DMFT. It improves upon the local and static interaction vertex included in TPSC, which cannot consistently describe low- and high-energy features simultaneously due to its static nature. For example, the vertices do not recover their bare values at large frequencies as they are renormalized by low-energy spin and charge fluctuations.

In this scheme, the effective momentum-dependent dynamical self-energy is given as the local DMFT self-energy Σ^{DMFT} combined with the nonlocal TPSC self-energy, namely,

$$\Sigma(k, i\omega_n) = \Sigma^{\text{TPSC}}(k, i\omega_n) - \frac{1}{N}\sum_{k'} \Sigma^{\text{TPSC}}(k', i\omega_n) + \Sigma^{\text{DMFT}}(i\omega_n), \tag{15}$$

where k is a reciprocal lattice vector in the first Brillouin zone, ω_n is the nth fermionic Matsubara frequency, and N is the number of k points. The idea of Eq. (15) was previously developed for a different many-body approach [23].

III. RESULTS

We consider the two-orbital Hubbard model given by Eq. (1) to facilitate comparison with the multiorbital TPSC formalism presented in Ref. [30]. The hopping terms are restricted to only nearest-neighbor hopping and to be orbital-diagonal $t_{\alpha\beta} = t_{\alpha\alpha}\delta_{\alpha\beta}$. The only coupling between the orbitals is via the interaction terms given by U and J. We consider the half-filled case with one electron per orbital per site. In the first part, we will discuss the effect of the DMFT-derived double-occupations on the TPSC two-particle quantities within $\langle nn\rangle_{\text{DMFT}}$-TPSC. These results apply in the same way to $\langle nn\rangle_{\text{DMFT}}$-TPSC+$\Sigma_{\text{DMFT}}$ as there is no feedback from the local DMFT self-energy on TPSC besides the inclusion of the DMFT double-occupations. The DMFT calculations are based on the ALPSCore continuous-time quantum Monte Carlo impurity solver in the hybridization expansion [88,89].

A. Double-occupations

In Table I, we show the double-occupations obtained from multiorbital TPSC compared to DMFT for $U/t = 3$, for moderate ($J = U/5$), and large ($J = U/3$) values of the Hund's coupling at different temperatures T/t. We find the general trend that the TPSC equal-orbital double-occupations are about 5–15% smaller than the ones obtained from DMFT indicating stronger local correlation effects in TPSC similar to the single-orbital case [23]. Furthermore, TPSC shows a monotonous increase as a function of temperature as it does not capture the reduction of the double-occupation induced by favoring localization to increase spin entropy [23,84,90]. We attribute this behavior in TPSC to the mean-field-like ansatz equation (6). Although this effect is observed in TPSC for weakly correlated systems [23], it is not captured in strongly correlated systems [28], such as in this case. Although DMFT obtains this reduction qualitatively, it is known to overestimate this effect [91]. For the same reason, we also observe a reversed temperature trend between TPSC and DMFT for $\langle n_{\alpha,\uparrow}n_{\beta,\uparrow}\rangle$. The remaining double-occupations follow qualitatively the same temperature dependence with TPSC double-occupations being, in general, 5–10% larger. Compared to moderate values of the Hund's coupling $U/J = 5$, we observe for larger values $U/J = 3$ the same trends, but the root search for determining the values of the spin vertex becomes increasingly unstable, which did not allow us to obtain converged results for temperatures below $T/t < 0.35$. Especially in such cases, a more reliable way of obtaining the double-occupations as input for the TPSC calculation, such as from a DMFT calculation is promising and will be explored in the next section.

TABLE I. Double occupations as obtained from TPSC and DMFT at $U/t = 3$ for different Hund's coupling J and temperatures T. Missing data points correspond to parameters where no TPSC convergence could be achieved.

$U/J = 5$	$\langle n_{\alpha,\uparrow}n_{\alpha,\downarrow}\rangle$		$\langle n_{\alpha,\uparrow}n_{\beta,\downarrow}\rangle$		$\langle n_{\alpha,\uparrow}n_{\beta,\uparrow}\rangle$	
T/t	DMFT	TPSC	DMFT	TPSC	DMFT	TPSC
0.5	0.1734	0.1571	0.2183	0.2361	0.2518	0.2692
0.4	0.1759	0.1562	0.2193	0.2367	0.2517	0.2714
0.3	0.1786	0.1541	0.2207	0.2376	0.2513	0.2759
0.25	0.1796	0.1502	0.2205	0.2387	0.2507	0.2826
$U/J = 3$	$\langle n_{\alpha,\uparrow}n_{\alpha,\downarrow}\rangle$		$\langle n_{\alpha,\uparrow}n_{\beta,\downarrow}\rangle$		$\langle n_{\alpha,\uparrow}n_{\beta,\uparrow}\rangle$	
T/t	DMFT	TPSC	DMFT	TPSC	DMFT	TPSC
0.5	0.1595	0.1477	0.2197	0.213	0.2697	0.2832
0.4	0.1614	0.1437	0.22204	0.213	0.2691	0.2899
0.3	0.1646		0.2213		0.2685	
0.25	0.1663		0.2220		0.2676	

B. Spin and charge vertices

As the effective local vertices in TPSC are determined by imposing local sum rules that depend on the double-occupations, the DMFT-derived double-occupations have a direct influence on the effective interaction vertices $\Gamma^{\text{sp/ch}}$ in $\langle nn\rangle_{\text{DMFT}}$-TPSC. In Fig. 1, we show the spin vertex Γ^{sp} as a function of interaction strength U/t for different values of U/J. In contrast to all the intra- and interorbital double-occupations, which show substantial differences between TPSC and DMFT, we observe a selective effect on the different elements of the spin vertex. Overall, the same

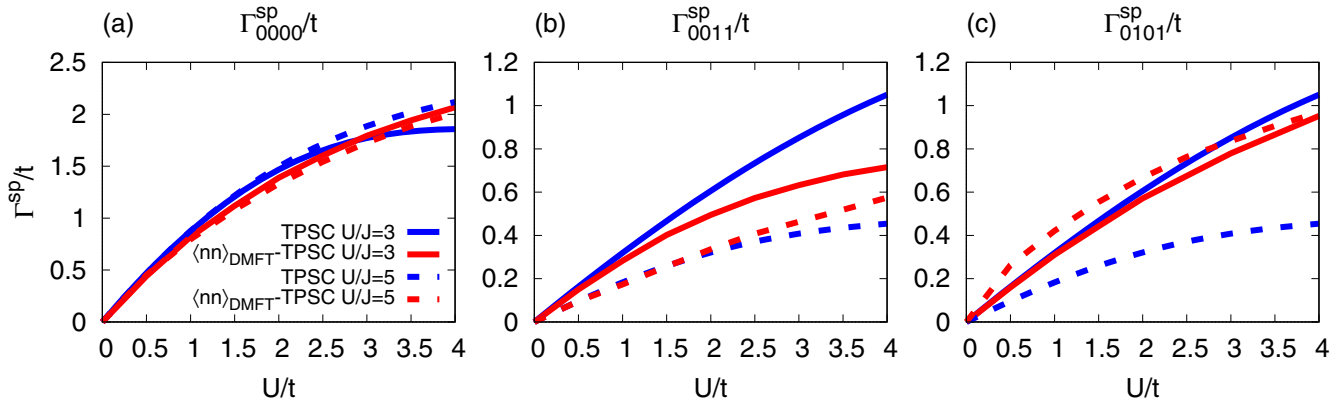

FIG. 1. Spin vertex components (a) $\Gamma^{sp}_{\alpha\alpha\alpha\alpha}$, (b) $\Gamma^{sp}_{\alpha\alpha\beta\beta}$, and (c) $\Gamma^{sp}_{\alpha\beta\alpha\beta}$ as a function of U/t for $U/J = 3$ (full lines) and $U/J = 5$ (dashed lines) within TPSC and $\langle nn\rangle_{\mathrm{DMFT}}$-TPSC. Although both methods show a similar dependence on U, we find a nontrivial effect of the DMFT double-occupations when included in TPSC: The off-diagonal vertex elements are increased for small Hund's coupling J but are reduced for large J with significant modification of the $\Gamma^{\mathrm{sp}}_{\alpha\beta\alpha\beta}$ element. This element is determined by its own sum rule in $\langle nn\rangle_{\mathrm{DMFT}}$-TPSC, in contrast to TPSC where it is set equal to $\Gamma^{\mathrm{sp}}_{\alpha\alpha\beta\beta}$. The remaining nonzero element $\Gamma^{sp}_{\alpha\beta\beta\alpha}$ is equal to $\Gamma^{sp}_{\alpha\beta\alpha\beta}$. TPSC data taken from Ref. [30].

functional dependence of Γ^{sp} on U/t as in TPSC is retained with Kanamori-Brueckner screening at larger interaction values. Although the diagonal elements $\Gamma^{\mathrm{sp}}_{\alpha\alpha\alpha\alpha}$ stay almost unchanged, the off-diagonal elements differ significantly, and the changes are sensitive to Hund's coupling J. For small J, the inclusion of the DMFT double-occupation leads to an increase in the effective spin vertex element, whereas, for large J, they are reduced compared to the TPSC value. The increase is especially pronounced in the $\alpha\beta\alpha\beta$ element for small J. We attribute this to the mean-field-like decoupling in the TPSC ansatz, which seems to perform better for larger values of J where, on average, the bare interaction elements are reduced. Most importantly, we observe that the $\Gamma^{\mathrm{sp}}_{\alpha\beta\alpha\beta}$ element, which in $\langle nn\rangle_{\mathrm{DMFT}}$-TPSC is now determined by its own sum rule, can differ up to a factor of 2 from the $\Gamma^{\mathrm{sp}}_{\alpha\alpha\beta\beta}$ element. This indicates that the ansatz $\Gamma^{\mathrm{sp}}_{\alpha\beta\alpha\beta} = \Gamma^{\mathrm{sp}}_{\alpha\alpha\beta\beta}$ in multiorbital TPSC due to a lack of sum rules constitutes a significant approximation and is not able to capture the renormalization of the off-diagonal spin vertex elements. In Fig. 2, we show the charge vertex Γ^{ch} obtained from TPSC and $\langle nn\rangle_{\mathrm{DMFT}}$-TPSC. Although the diagonal elements $\Gamma^{\mathrm{ch}}_{\alpha\alpha\alpha\alpha}$ [Fig. 2(a)] monotonously increase as a function of U and show only minor differences between the two approaches, we find the most significant improvement in the $\Gamma^{\mathrm{ch}}_{\alpha\alpha\beta\beta}$ elements [Fig. 2(b)]: The large negative values for the charge vertices $\Gamma^{\mathrm{ch}}_{\alpha\alpha\beta\beta}$ observed in TPSC are absent in $\langle nn\rangle_{\mathrm{DMFT}}$-TPSC, which resolves the problem of unphysical negative spectral weight contributions to the self-energy at larger values of U/t [30]. The $\Gamma^{\mathrm{ch}}_{\alpha\beta\alpha\beta}$ element [Fig. 2(c)], on the other hand, is reduced compared to TPSC, which is likely due to a previous compensation effect with the smaller or negative $\Gamma^{\mathrm{ch}}_{\alpha\alpha\beta\beta}$ in order to fulfill the corresponding sum rule, which required larger values of $\Gamma^{\mathrm{ch}}_{\alpha\beta\alpha\beta}$. Still, we observe small negative values of $\Gamma^{\mathrm{ch}}_{\alpha\beta\alpha\beta}$ at weak interaction, but they are negligible due to their small relative magnitude $|\Gamma^{\mathrm{ch}}_{\alpha\beta\alpha\beta}|/U \approx 10^{-2}$.

These results suggest that the DMFT double-occupations can provide a significant improvement over the multiorbital

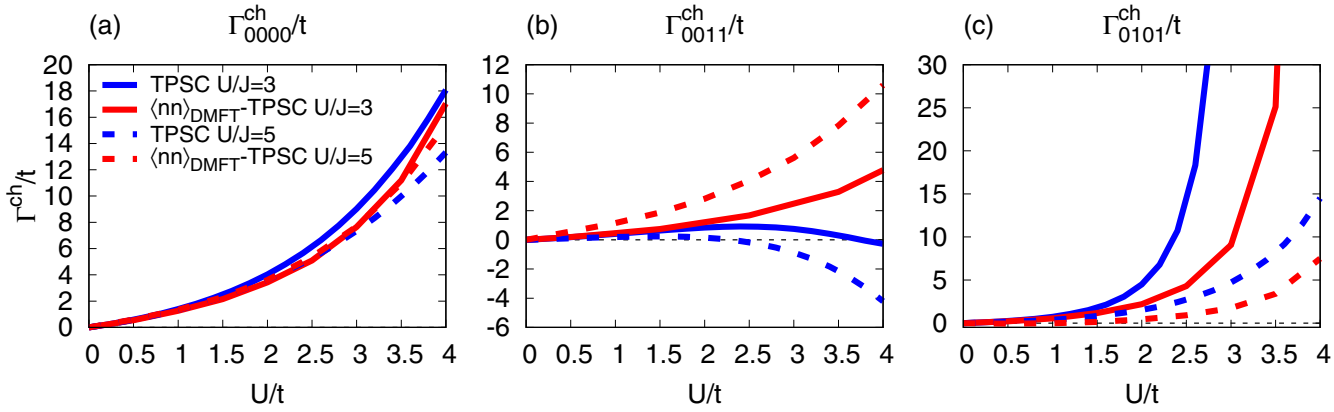

FIG. 2. Charge vertex components (a) $\Gamma^{\mathrm{ch}}_{\alpha\alpha\alpha\alpha}$, (b) $\Gamma^{\mathrm{ch}}_{\alpha\alpha\beta\beta}$, and (c) $\Gamma^{\mathrm{ch}}_{\alpha\beta\alpha\beta}$ as a function of U/t for $U/J = 3$ (dashed lines) and $U/J = 5$ (full lines) within TPSC (blue) and $\langle nn\rangle_{\mathrm{DMFT}}$-TPSC (red). Although the inclusion of the DMFT double-occupations only leads to a small increase in the diagonal vertex elements, the $\Gamma^{\mathrm{ch}}_{\alpha\alpha\beta\beta}$ elements, which in TPSC are negative and lead to unphysical solutions, become strictly positive. The $\Gamma^{\mathrm{ch}}_{\alpha\beta\alpha\beta}$ elements are reduced significantly in $\langle nn\rangle_{\mathrm{DMFT}}$-TPSC with negligible negative values at small interactions. TPSC results are taken from Ref. [30].

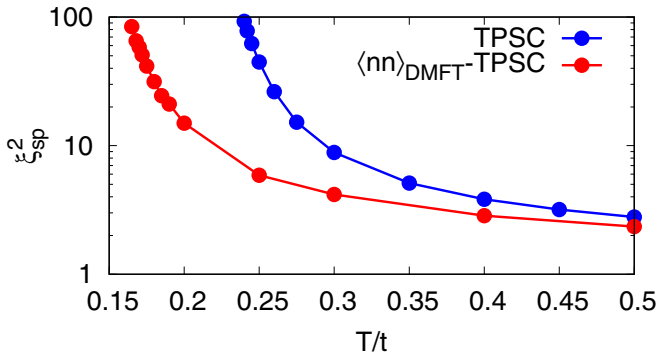

FIG. 3. Antiferromagnetic spin-correlation length ξ^2_{sp} as a function of temperature T/t at $U/t = 3, U/J = 5$. Although TPSC fulfills the Mermin-Wagner theorem with the divergence at $T = 0$, it overestimates the spin-correlation length. $\langle nn\rangle_{\text{DMFT}}$-TPSC obtains a reduced correlation length for all temperatures considered.

TPSC ansatz equations in the multiorbital case as they result in physical vertices, in contrast to the multiorbital TPSC approach. Although, in general, we cannot exclude the existence of certain scenarios where the vertex elements can become negative and large (as likely might be the case where the approximation of a static vertex is not appropriate), we expect this to be a general result for many systems of interest, and that $\langle nn\rangle_{\text{DMFT}}$-TPSC provides access to more strongly correlated systems that were previously out of reach within multiorbital TPSC.

C. Antiferromagnetic spin fluctuations

In order to assess the effect of the DMFT-derived double-occupations on the spin fluctuations in TPSC, we define the antiferromagnetic spin-correlation length as the ratio of the spin and bare susceptibility at the M point,

$$\xi^2_{\text{sp}} := \frac{\chi^{\text{sp}}_{\alpha\alpha\alpha\alpha}[\vec{q} = (\pi, \pi), \omega = 0]}{\chi^0[\vec{q} = (\pi, \pi), \omega = 0]}. \tag{16}$$

Figure 3 shows ξ^2_{sp} at $U/t = 3$ and $U/J = 5$ as a function of temperature. The spin-correlation length increases upon lowering the temperature, representing the increasing antiferromagnetic fluctuations in the two-dimensional Hubbard model [23,82] but only diverges at $T = 0$ as TPSC obeys the Mermin-Wagner theorem. We observe that the spin correlation length in $\langle nn\rangle_{\text{DMFT}}$-TPSC is smaller than in multiorbital TPSC at the same temperature up to more than an order of magnitude at lower temperatures. This is indicative for the overestimation of the strength of spin fluctuations in TPSC [23,29], which is significantly improved when deriving the spin vertex from the DMFT double-occupations (see Table I). In fact, $\langle nn\rangle_{\text{DMFT}}$-TPSC can also be seen as an effective way of mimicking frequency-dependent vertex corrections in TPSC via the double-occupations. A similar improvement can be seen in TPSC+ [23,92], which includes effective dynamical vertex corrections by a feedback of the self-energy into the propagators. We note that this behavior is dependent on the model parameters as we find that for a given temperature $\langle nn\rangle_{\text{DMFT}}$-TPSC can lead both to a reduction of the antiferromagnetic correlations at small values of U and to an enhancement at larger values of U as will be shown in the next section.

D. Susceptibilities

In the following sections, we will perform a benchmark of the $\langle nn\rangle_{\text{DMFT}}$-TPSC and $\langle nn\rangle_{\text{DMFT}}$-TPSC+$\Sigma_{\text{DMFT}}$ approach on a two-orbital Hubbard model and compare our results to the D-TRILEX approach [59]. D-TRILEX is an approximation to the dual boson method and has recently been extended to multiorbital systems [62]. It treats charge and spin fluctuations on the same footing, and by the inclusion of the dynamical but local three-point vertex, is able to describe nonlocal correlation and screening effects in strongly interacting systems. This makes it a reasonable reference method for our improved TPSC schemes, which work with a simplified static and local two-point vertex.

In the following, we consider the half-filled two-orbital Hubbard square lattice at temperature $T/t = 0.5$ with an orbital-dependent nearest-neighbor hopping,

$$t_{00} = 1.0, \quad t_{11} = 0.75, \tag{17}$$

where the bandwidth of the second orbital is reduced by 25%. In Fig. 4, we show the momentum-resolved summed spin and charge susceptibilities,

$$\chi^{\text{ch/sp}}_{\text{sum}}(q, 0) := \sum_{\alpha,\beta} \chi^{\text{ch/sp}}_{\alpha\alpha\beta\beta}(q, 0) \tag{18}$$

for $U/t = 2, 4, 6$ and $U/J = 4$ obtained within multiorbital TPSC and $\langle nn\rangle_{\text{DMFT}}$-TPSC, and compare them to the D-TRILEX results from Ref. [62]. In general, we find good qualitative and quantitative agreement among the three methods for small interactions in both the charge and spin susceptibilities [Figs. 4(a) and 4(d)]. They exhibit pronounced peaks at the $M = (\pi, \pi)$ point, corresponding to spin and charge fluctuations with wave-vector $\vec{q} = (\pi, \pi)$ with the dominating spin fluctuations indicating antiferromagnetic order as the main instability of the system. All methods show a reduction of the charge susceptibility and increase in the spin susceptibility for increasing interaction $U/t = 2 \cdots 6$. Although the differences at $U/t = 2$ between TPSC and $\langle nn\rangle_{\text{DMFT}}$-TPSC are small, one clearly observes a shift towards the D-TRILEX result when using the DMFT-derived double-occupations, bringing the spin susceptibility of $\langle nn\rangle_{\text{DMFT}}$-TPSC in almost perfect agreement with D-TRILEX. At stronger interactions, we observe that multiorbital TPSC significantly overestimates the charge susceptibility but underestimates the spin susceptibility, and increasingly starts to deviate from the D-TRILEX result. On the other hand, $\langle nn\rangle_{\text{DMFT}}$-TPSC always shows the tendency to correct the difference to D-TRILEX but overestimates the reduction of the charge susceptibility and the enhancement of the spin susceptibility for larger interactions [Figs. 4(b), 4(c) and 4(f)]. Although multiorbital TPSC is not able to capture the Mott transition in either orbital and also obtains a charge susceptibility that is significantly too large at $U/t = 6$, the DMFT double-occupations effectively encode the insulating nature of the system in $\langle nn\rangle_{\text{DMFT}}$-TPSC, which shows an almost vanishing charge susceptibility at this interaction value.

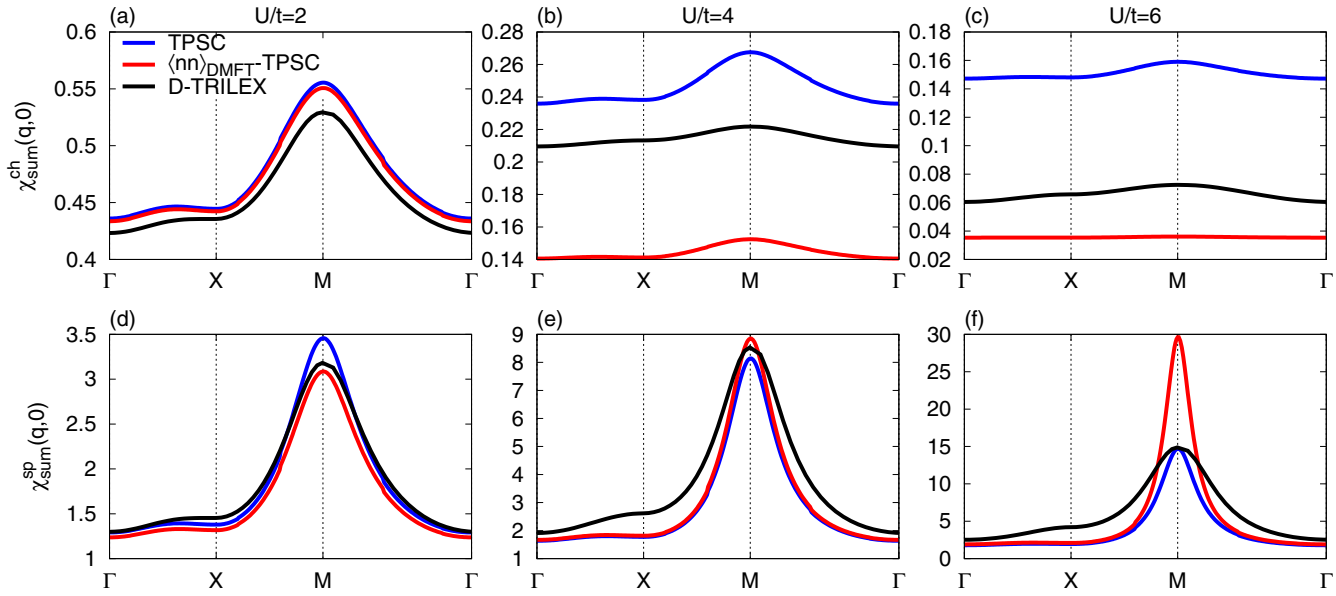

FIG. 4. Summed charge (upper panels) and spin (lower panels) susceptibilities $\sum_{\alpha,\beta}\chi^{\mathrm{sp/ch}}_{\alpha\alpha\beta\beta}(q,0)$ along Γ-X-M-Γ for (a), (d) $U/t=2$, (b) and (e) $U/t=4$, (c) and (f) $U/t=6$ and $U/J=4$ obtained from TPSC, $\langle nn\rangle_{\mathrm{DMFT}}$-TPSC, and D-TRILEX. In both cases, we observe the suppression/enhancement of charge/spin fluctuations with increasing U/t. Although TPSC underestimates this trend, inclusion of the DMFT double-occupations within $\langle nn\rangle_{\mathrm{DMFT}}$-TPSC+$\Sigma_{\mathrm{DMFT}}$ lead to an improved agreement with D-TRILEX at moderate interaction values. For strong interactions, the suppression/enhancement of charge/spin fluctuations is overestimated in $\langle nn\rangle_{\mathrm{DMFT}}$-TPSC+$\Sigma_{\mathrm{DMFT}}$. D-TRILEX results are taken from Ref. [62].

E. Spectral function

So far, we have only discussed quantities, such as the double-occupation, effective vertices or susceptibilities within $\langle nn\rangle_{\mathrm{DMFT}}$-TPSC. As these quantities only depend on the noninteracting Green's function, bare interaction and DMFT double-occupations, they are not affected by a replacement of the local TPSC self-energy with the DMFT impurity self-energy as proposed for $\langle nn\rangle_{\mathrm{DMFT}}$-TPSC+$\Sigma_{\mathrm{DMFT}}$. On the other hand, the single-particle local spectral function,

$$A(\omega)=\frac{-1}{\pi N}\sum_{k}\mathrm{Im}[\omega+i0^{+}-H_0(k)-\Sigma(k,\omega)]^{-1} \quad (19)$$

will be affected by the replacement as it directly depends on the final self-energy. For the same two-orbital Hubbard model as in the previous section, we compare the two different methods with TPSC and D-TRILEX [62] at different interactions for $U/J=4$ in Fig. 5. Analytic continuation from the imaginary to the real frequency axis has been performed by using the maximum entropy formalism [88,93,94]. In agreement with D-TRILEX we find the orbital with the larger bandwidth to be less correlated than the one with the narrow bandwidth (see Fig. 5), and we observe an overall increase in correlation effects as the interaction is increased. All TPSC-related methods differ considerably from each other: We obtain that multiorbital TPSC underestimates the correlation strength the most and, thus, shows the largest difference to the D-TRILEX results for all interaction values in both orbitals. The approach is also not able to capture the large reduction of spectral weight at the Fermi level in the first orbital and a Mott transition in the second orbital at $U/t=7$ [Figs. 5(e) and 5(f)]. $\langle nn\rangle_{\mathrm{DMFT}}$-TPSC, on the other hand, provides a considerable improvement over TPSC, capturing the reduction of spectral weight qualitatively but still underestimates the correlation strength. The best agreement with the D-TRILEX benchmark is found for $\langle nn\rangle_{\mathrm{DMFT}}$-TPSC+$\Sigma_{\mathrm{DMFT}}$, which is able to capture the Mott transition and shows close agreement for all parameters considered, albeit a remaining underestimation of the correlation strength. These results show that the incorporation of more accurate double-occupations within the $\langle nn\rangle_{\mathrm{DMFT}}$-TPSC approach already leads to a notable improvement over TPSC. Still, for strongly correlated systems, the static TPSC vertex entering the self-energy remains a major limitation as expected. This limitation can be drastically improved by a combination with the DMFT impurity self-energy in $\langle nn\rangle_{\mathrm{DMFT}}$-TPSC+$\Sigma_{\mathrm{DMFT}}$, providing access to the Mott-insulating phase, which was previously not accessible in TPSC.

IV. CONCLUSION

In this paper, we have presented two extensions of the multiorbital TPSC approach [30] that are based on incorporating local quantities, which can be obtained with higher precision from a DMFT calculation in the TPSC formalism. The first extension, called $\langle nn\rangle_{\mathrm{DMFT}}$-TPSC, consists in replacing the usual ansatz equations for the double-occupations in TPSC by the double-occupations sampled in a DMFT calculation for the same system. As the TPSC ansatz is based on a Hartree-Fock-like decoupling, this avoids additional approximations in the determination of the double-occupations, which are needed for the determination of the effective spin and charge vertices in TPSC. We found this approach to be highly successful specifically for the multiorbital form of TPSC as it removed the negative divergences of the charge vertex Γ^{ch} observed in the multorbital TPSC approach [30]. Additionally, certain

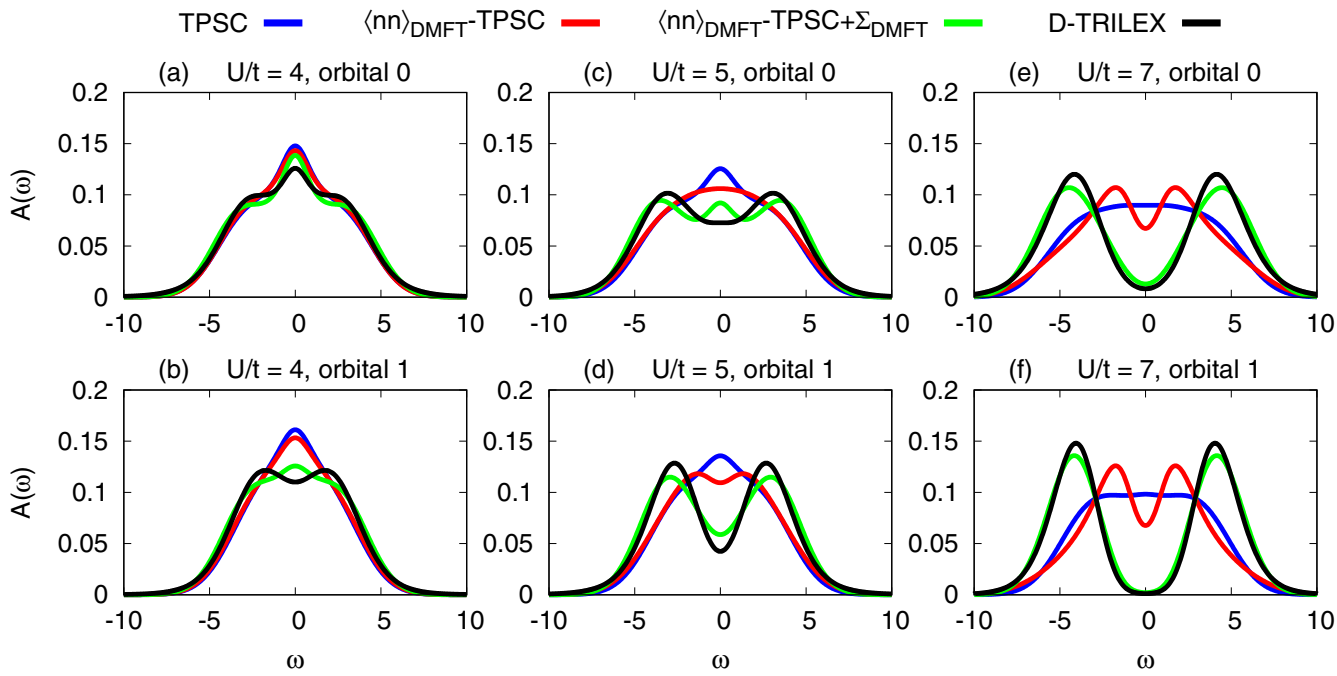

FIG. 5. The local spectral function $A(\omega)$ obtained for the two-orbital Hubbard model (see the main text) from TPSC (blue), $\langle nn\rangle_{\text{DMFT}}$-TPSC (red), $\langle nn\rangle_{\text{DMFT}}$-TPSC+$\Sigma_{\text{DMFT}}$ (green), and D-TRILEX (black) for interaction values (a) and (b) $U/t = 4$, (c) and (d) $U/t = 5$, and (e) and (f) $U/t = 7$. TPSC underestimates the correlation strength for all parameters considered and is not able to obtain the reduction of spectral weight at the Fermi level for stronger interactions. Incorporating the DMFT double-occupations in $\langle nn\rangle_{\text{DMFT}}$-TPSC provides a notable improvement over TPSC, whereas only $\langle nn\rangle_{\text{DMFT}}$-TPSC+$\Sigma_{\text{DMFT}}$ is able to access the Mott-insulating phase in the second orbital and obtains a qualitative agreement with the D-TRILEX result. D-TRILEX results are taken from Ref. [62].

interorbital elements of the effective spin vertex, which previously were determined by symmetries only valid for the bare interaction vertex, can be determined explicitly, and indeed show an expected deviation from the bare interaction case. This extension also provides access to lower temperatures that were previously inaccessible in TPSC as divergences in the spin vertex are shifted to lower temperatures. Furthermore, it allows for the inclusion of the transversal particle-hole channel, which restores crossing symmetry in the vertex functions. Nevertheless, we note that the double-occupations are influenced by nonlocal correlations, which are not taken into account in DMFT, in particular, in regions where strong order parameter fluctuations prevail [95,96]. See Appendix A for further discussion on the double-occupations and Appendix B for a discussion on the internal consistency between single- and two-particle objects.

In the second proposed extension, we replace the local part of the the TPSC self-energy by the impurity self-energy of DMFT, called $\langle nn\rangle_{\text{DMFT}}$-TPSC+$\Sigma_{\text{DMFT}}$. This approach improves upon the static vertex included in TPSC by effectively incorporating a dynamical DMFT vertex in the local self-energy, whereas retaining nontrivial momentum-dependent correlation effects from TPSC at low computational costs. We found this approach to provide further improved agreement with other many-body methods especially for local one-particle quantities, such as the local spectral function. This approach also extends the applicability of TPSC to systems with strong correlations as it is able to access the Mott-insulating phase, previously inaccessible in multiorbital TPSC. We note here that by replacing the local part of the self-energy, we still have contributions from nonlocal correlation effects. From the diagrammatic point of view our quantity is, therefore, only semilocal. An alternative approach can be constructed by means of the local Dyson equation where the local Green's function is used to obtain the local self-energy, which allow us to subtract all nonlocal correlation effects, but, on the other hand, does not yield the exact DMFT result in the limit of infinite connectivity.

These results show the potential of combining TPSC with DMFT for both local and nonocal quantities and opens up the door towards further developments, such as fully self-consistent TPSC+DMFT calculations and further applications to real materials.

ACKNOWLEDGMENTS

We thank A.-M. Tremblay, C.-A. Gauvin-Ndiaye, N. Martin, and O. Gingras for useful discussions. We acknowledge support from the Deutsche Forschungsgemeinschaft (DFG, German Research Foundation) through TRR 288-422213477 (Project No. B05) (A.R., R.V.) and through FOR 5249-449872909 (Project No. P4) (R.V.).

APPENDIX A: DOUBLE-OCCUPATIONS

In order to compare the resulting values for the double-occupations for the different approaches and the influence of nonlocal correlations, we show the double-occupations from TPSC, DMFT, and D-TRILEX in Fig. 6. As discussed in the main text, the deviation between the TPSC

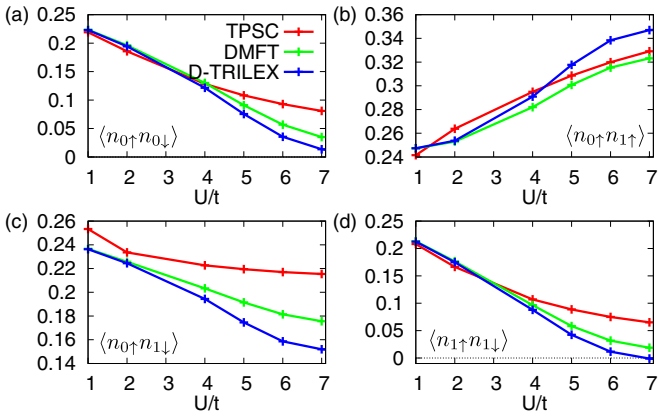

FIG. 6. Comparison of the double-occupations for the model described in Sec. III D. We observe a small difference between all methods at low interaction strength ($U < 3t$) but larger differences at higher interaction strength where nonlocal correlations become significant. In general, the DMFT-derived double-occupations show a closer agreement with the D-TRILEX result than TPSC except for the high-spin interorbital configuration, indicating that the DMFT result can serve as a possible improved starting point for the determination of the effective TPSC vertices. The results for the D-TRILEX double-occupancies have been provided by the authors of Ref. [62].

and the DMFT double-occupations is small at weak interaction strength ($U/t < 3$) but becomes larger for stronger interactions, as TPSC is not able to capture the Mott-insulator phase. In general, the deviation between the DMFT and the D-TRILEX double-occupations is smaller, indicating that indeed the DMFT double-occupations are a better starting point than the TPSC-derived ones. When nonlocal correlations become strong at larger interaction values, the DMFT and D-TRILEX results also start to differ, with the general trend that D-TRILEX obtains a larger correlation strength, i.e., reduced low-spin double-occupations and enhanced high-spin configurations.

APPENDIX B: INTERNAL CONSISTENCY CHECK

In the original TPSC formulation [70] the $\mathrm{tr}(\Sigma G)$ sum rule,

$$\begin{aligned}\mathrm{tr}(\Sigma G)_{\beta,\sigma} &= \sum_{\alpha} U_{\alpha\beta}\langle n_{\alpha,-\sigma}n_{\beta,\sigma}\rangle + \sum_{\substack{\alpha\\ \alpha\neq\beta}}(U_{\alpha\beta}-J_{\alpha\beta})\langle n_{\alpha,\sigma}n_{\beta,\sigma}\rangle \\ &\quad - \sum_{\substack{\alpha\\ \alpha\neq\beta}} J_{\alpha\beta}\left(\langle n_{\alpha,\sigma}n_{\beta,\sigma}\rangle - \langle n_{\alpha,-\sigma}n_{\beta,\sigma}\rangle\right) \\ &\quad - \frac{1}{\tilde{\beta}N_{\vec{q}}}\sum_{\substack{q,\alpha\\ \alpha\neq\beta}}\frac{J_{\alpha\beta}}{2}\left[\chi^{\mathrm{sp}}_{\beta\alpha\alpha\beta}(q) - \chi^{\mathrm{ch}}_{\beta\alpha\alpha\beta}(q)\right] \end{aligned} \tag{B1}$$

is used as a mean of consistency check between single-particle and two-particle objects. The same relation can also be established in the multiorbital case [30]. Here, we investigate how this consistency changes between the different TPSC extensions. The comparison is again performed for the model presented in Sec. III D, where we show the results in Table II.

TABLE II. Relative error in the $\mathrm{tr}(\Sigma G)$-sum rule obtained from TPSC, $\langle nn\rangle_{\mathrm{DMFT}}$-TPSC, $\langle nn\rangle_{\mathrm{DMFT}}$-TPSC+$\Sigma_{\mathrm{DMFT}}$. Although the error increases when using only the DMFT double-occupations, we observe that this is again compensated when also including the DMFT self-energy, leading to a reduction of the error.

U/t	TPSC	$\langle nn\rangle_{\mathrm{DMFT}}$-TPSC	$\langle nn\rangle_{\mathrm{DMFT}}$-TPSC+$\Sigma_{\mathrm{DMFT}}$
		Orbital 0	
4	6.129×10^{-2}	1.015×10^{-1}	3.142×10^{-2}
5	9.658×10^{-2}	2.240×10^{-1}	8.675×10^{-3}
7	2.364×10^{-1}	6.230×10^{-1}	2.408×10^{-1}
		Orbital 1	
4	9.854×10^{-2}	1.666×10^{-1}	2.3988×10^{-2}
5	1.467×10^{-1}	3.460×10^{-1}	2.9320×10^{-2}
7	3.089×10^{-1}	7.865×10^{-1}	2.2499×10^{-1}

We observe an increase in the relative error between the left-hand and right-hand side of the $\mathrm{tr}(\Sigma G)$-sum rule when using $\langle nn\rangle_{\mathrm{DMFT}}$-TPSC instead of TPSC. This effect can be reversed when the DMFT self-energy is also included. We attribute this observation to an additional inconsistency when using the DMFT double-occupations without inclusion of the DMFT self-energy. Only when all the correlation effects that are accounted for in DMFT are present on both sides of the sum rule, namely, the double-occupations and the self-energy, the error decreases again.

APPENDIX C: NODAL/ANTINODAL SPECTRAL FUNCTION

To demonstrate the resulting effect of the combined TPSC and DMFT scheme on the Fermi surface and possible emergence of a pseudogap via a the momentum-dependent self-energy, we show the analytically continued spectral function at the nodal $(\pi/2, \pi/2)$ and antinodal $(\pi, 0)$ points in Fig. 7 for a fixed value of the interaction $U/t = 5$. We observe a larger suppression of spectral weight at the antinodal point compared to the nodal point, which originates from the larger imaginary part of the momentum-dependent self-energy at the antinodal point, indicative of a tendency to form a pseudogap. The relative suppression is similar in all schemes, i.e., we find that the momentum separation of the correlation effects at the nodal and antinodal points is not significantly affected by using the DMFT double-occupancies in the DMFT scheme. The replacement of the local TPSC self-energy by the DMFT self-energy does not modify the overall relative momentum dependence, therefore, in all schemes the momentum dependence of the self-energy is mostly governed by the original pure TPSC result.

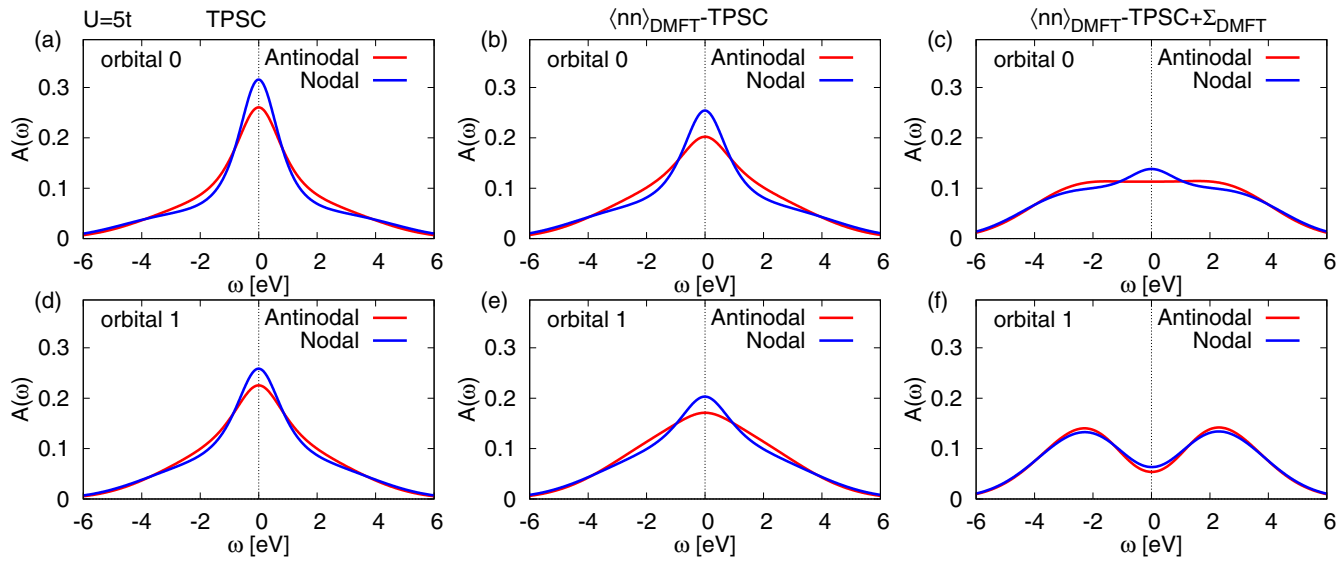

FIG. 7. Spectral function at the nodal $(\pi/2, \pi/2)$ and antinodal $(\pi, 0)$ points, calculated using the three approaches TPSC, $\langle nn\rangle_{\mathrm{DMFT}}$-TPSC and $\langle nn\rangle_{\mathrm{DMFT}}$-TPSC+$\Sigma_{\mathrm{DMFT}}$, for interaction strength $U/t = 5$ and temperature $T/t = 0.5$. The spectral function at the antinodal point shows a greater suppression of spectral weight than at the nodal point, representative of the tendency to form a pseudogap. Due to a rather high temperature, the momentum dependence is not very pronounced.

[1] P. W. Anderson, The resonating valence bond state in La_2CuO_4 and superconductivity, Science **235**, 1196 (1987).

[2] G. Kotliar and J. Liu, Superexchange mechanism and d-wave superconductivity, Phys. Rev. B **38**, 5142 (1988).

[3] P. A. Lee, N. Nagaosa, and X.-G. Wen, Doping a mott insulator: Physics of high-temperature superconductivity, Rev. Mod. Phys. **78**, 17 (2006).

[4] C. Honerkamp, Density Waves and Cooper Pairing on the Honeycomb Lattice, Phys. Rev. Lett. **100**, 146404 (2008).

[5] S. V. Borisenko, V. B. Zabolotnyy, D. V. Evtushinsky, T. K. Kim, I. V. Morozov, A. N. Yaresko, A. A. Kordyuk, G. Behr, A. Vasiliev, R. Follath, and B. Büchner, Superconductivity without Nesting in LiFeAs, Phys. Rev. Lett. **105**, 067002 (2010).

[6] F. Wang and D.-H. Lee, The electron-pairing mechanism of iron-based superconductors, Science **332**, 200 (2011).

[7] M. R. Norman, The challenge of unconventional superconductivity, Science **332**, 196 (2011).

[8] D. Jerome, Organic superconductors: When correlations and magnetism walk in, J. Supercond. Novel Magn. **25**, 633 (2012).

[9] F. Steglich and S. Wirth, Foundations of heavy-fermion superconductivity: Lattice kondo effect and mott physics, Rep. Prog. Phys. **79**, 084502 (2016).

[10] D. Aoki, K. Ishida, and J. Flouquet, Review of u-based ferromagnetic superconductors: Comparison between UGe_2, URhGe, and UCoGe, J. Phys. Soc. Jpn. **88**, 022001 (2019).

[11] L. Balents, Spin liquids in frustrated magnets, Nature (London) **464**, 199 (2010).

[12] W. Witczak-Krempa, G. Chen, Y. B. Kim, and L. Balents, Correlated quantum phenomena in the strong spin-orbit regime, Annu. Rev. Condens. Matter Phys. **5**, 57 (2014).

[13] M. R. Norman, Colloquium: Herbertsmithite and the search for the quantum spin liquid, Rev. Mod. Phys. **88**, 041002 (2016).

[14] L. Savary and L. Balents, Quantum spin liquids: A review, Rep. Prog. Phys. **80**, 016502 (2017).

[15] Y. Zhou, K. Kanoda, and T.-K. Ng, Quantum spin liquid states, Rev. Mod. Phys. **89**, 025003 (2017).

[16] K. Riedl, R. Valentí, and S. M. Winter, Critical spin liquid versus valence-bond glass in a triangular-lattice organic antiferromagnet, Nat. Commun. **10**, 2561 (2019).

[17] H. Takagi, T. Takayama, G. Jackeli, G. Khaliullin, and S. E. Nagler, Concept and realization of kitaev quantum spin liquids, Nat. Rev. Phys. **1**, 264 (2019).

[18] J. Hubbard, Electron correlations in narrow energy bands, Proc. R. Soc. London A **276**, 238 (1963).

[19] J. Kanamori, Electron correlation and ferromagnetism of transition metals, Prog. Theor. Phys. **30**, 275 (1963).

[20] M. C. Gutzwiller, Effect of Correlation on the Ferromagnetism of Transition Metals, Phys. Rev. Lett. **10**, 159 (1963).

[21] G. Rohringer, H. Hafermann, A. Toschi, A. A. Katanin, A. E. Antipov, M. I. Katsnelson, A. I. Lichtenstein, A. N. Rubtsov, and K. Held, Diagrammatic routes to nonlocal correlations beyond dynamical mean field theory, Rev. Mod. Phys. **90**, 025003 (2018).

[22] E. Pavarini and S. Zhang (eds.), *Many-Body Methods for Real Materials*, Schriften des Forschungszentrums Jülich Modeling and Simulation, Vol. 9, Autumn School on Correlated Electrons, Jülich (Germany), 16 September 2019-20 September 2019 (Forschungszentrum Jülich GmbH Zentralbibliothek, Verlag, Jülich, 2019).

[23] T. Schäfer, N. Wentzell, F. Šimkovic, Y.-Y. He, C. Hille, M. Klett, C. J. Eckhardt, B. Arzhang, V. Harkov, F.-M. Le Régent, A. Kirsch, Y. Wang, A. J. Kim, E. Kozik, E. A. Stepanov, A. Kauch, S. Andergassen, P. Hansmann, D. Rohe, Y. M. Vilk *et al.* Tracking the Footprints of Spin

Fluctuations: A MultiMethod, MultiMessenger Study of the Two-Dimensional Hubbard Model, Phys. Rev. X **11**, 011058 (2021).
[24] M. Qin, T. Schäfer, S. Andergassen, P. Corboz, and E. Gull, The Hubbard model: A computational perspective, Annu. Rev. Condens. Matter Phys. **13**, 275 (2022).
[25] W. Metzner and D. Vollhardt, Correlated Lattice Fermions in $d = \infty$ Dimensions, Phys. Rev. Lett. **62**, 324 (1989).
[26] A. Georges and G. Kotliar, Hubbard model in infinite dimensions, Phys. Rev. B **45**, 6479 (1992).
[27] A. Georges, G. Kotliar, W. Krauth, and M. J. Rozenberg, Dynamical mean-field theory of strongly correlated fermion systems and the limit of infinite dimensions, Rev. Mod. Phys. **68**, 13 (1996).
[28] Y. M. Vilk, Shadow features and shadow bands in the paramagnetic state of cuprate superconductors, Phys. Rev. B **55**, 3870 (1997).
[29] A.-M. S. Tremblay, Two-particle-self-consistent approach for the Hubbard model, in *Strongly Correlated Systems: Theoretical Methods*, edited by A. Avella and F. Mancini (Springer, Berlin/Heidelberg, 2012), pp. 409–453.
[30] K. Zantout, S. Backes, and R. Valentí, Two-particle self-consistent method for the multi-orbital Hubbard model, Ann. Der Phys. **533**, 2000399 (2021).
[31] G. Kotliar and D. Vollhardt, Strongly correlated materials: Insights from dynamical mean-field theory, Phys. Today **57**(3), 53 (2004).
[32] S. Biermann, A. Poteryaev, A. I. Lichtenstein, and A. Georges, Dynamical Singlets and Correlation-Assisted Peierls Transition in vo_2, Phys. Rev. Lett. **94**, 026404 (2005).
[33] G. Kotliar, S. Y. Savrasov, K. Haule, V. S. Oudovenko, O. Parcollet, and C. A. Marianetti, Electronic structure calculations with dynamical mean-field theory, Rev. Mod. Phys. **78**, 865 (2006).
[34] A. Georges, L. d. Medici, and J. Mravlje, Strong correlations from Hund's coupling, Annu. Rev. Condens. Matter Phys. **4**, 137 (2013).
[35] D. Vollhardt, Dynamical mean-field theory of strongly correlated electron systems, in *Proceedings of the International Conference on Strongly Correlated Electron Systems (SCES2019)* (J. Phys. Soc. Jpn., Tokyo, 2020).
[36] M. R. Norman, H. Ding, M. Randeria, J. C. Campuzano, T. Yokoya, T. Takeuchi, T. Takahashi, T. Mochiku, K. Kadowaki, P. Guptasarma, and D. G. Hinks, Destruction of the fermi surface in underdoped high tc superconductors, Nature (London) **392**, 157 (1997).
[37] F. Ronning, C. Kim, D. L. Feng, D. S. Marshall, A. G. Loeser, L. L. Miller, J. N. Eckstein, I. Bozovic, and Z.-X. Shen, Photoemission evidence for a remnant fermi surface and a d-wave-like dispersion in insulating $Ca_2CuO_2Cl_2$, Science **282**, 2067 (1998).
[38] M. Imada, A. Fujimori, and Y. Tokura, Metal-insulator transitions, Rev. Mod. Phys. **70**, 1039 (1998).
[39] A. A. Kordyuk, Pseudogap from arpes experiment: Three gaps in cuprates and topological superconductivity (review article), Low Temp. Phys. **41**, 319 (2015).
[40] M. H. Hettler, A. N. Tahvildar-Zadeh, M. Jarrell, T. Pruschke, and H. R. Krishnamurthy, Nonlocal dynamical correlations of strongly interacting electron systems, Phys. Rev. B **58**, R7475(R) (1998).
[41] M. H. Hettler, M. Mukherjee, M. Jarrell, and H. R. Krishnamurthy, Dynamical cluster approximation: Nonlocal dynamics of correlated electron systems, Phys. Rev. B **61**, 12739 (2000).
[42] T. Maier, M. Jarrell, T. Pruschke, and J. Keller, A non-crossing approximation for the study of intersite correlations, Eur. Phys. J. B **13**, 613 (2000).
[43] G. Kotliar, S. Y. Savrasov, G. Pálsson, and G. Biroli, Cellular Dynamical Mean Field Approach to Strongly Correlated Systems, Phys. Rev. Lett. **87**, 186401 (2001).
[44] T. A. Maier, M. Jarrell, T. Pruschke, and M. Hettler, Quantum cluster theories, Rev. Mod. Phys. **77**, 1027 (2005).
[45] H. Park, K. Haule, and G. Kotliar, Cluster Dynamical Mean Field Theory of the Mott Transition, Phys. Rev. Lett. **101**, 186403 (2008).
[46] S. Biermann, F. Aryasetiawan, and A. Georges, First-Principles Approach to the Electronic Structure of Strongly Correlated Systems: Combining the *gw* Approximation and Dynamical Mean-Field Theory, Phys. Rev. Lett. **90**, 086402 (2003).
[47] P. Sun and G. Kotliar, Many-Body Approximation Scheme beyond GW, Phys. Rev. Lett. **92**, 196402 (2004).
[48] T. Ayral, P. Werner, and S. Biermann, Spectral Properties of Correlated Materials: Local Vertex and Nonlocal Two-Particle Correlations from Combined *gw* and Dynamical Mean Field Theory, Phys. Rev. Lett. **109**, 226401 (2012).
[49] S. Biermann, Dynamical screening effects in correlated electron materials—a progress report on combined many-body perturbation and dynamical mean field theory: 'GW + DMFT', J. Phys.: Condens. Matter **26**, 173202 (2014).
[50] L. Boehnke, F. Nilsson, F. Aryasetiawan, and P. Werner, When strong correlations become weak: Consistent merging of *gw* and dmft, Phys. Rev. B **94**, 201106(R) (2016).
[51] S. Backes, J.-H. Sim, and S. Biermann, Nonlocal correlation effects in fermionic many-body systems: Overcoming the noncausality problem, Phys. Rev. B **105**, 245115 (2022).
[52] A. Toschi, A. A. Katanin, and K. Held, Dynamical vertex approximation: A step beyond dynamical mean-field theory, Phys. Rev. B **75**, 045118 (2007).
[53] K. Held, A. A. Katanin, and A. Toschi, Dynamical Vertex Approximation: An Introduction, Prog. Theor. Phys. Suppl. **176**, 117 (2008).
[54] A. Galler, J. Kaufmann, P. Gunacker, M. Pickem, P. Thunström, J. M. Tomczak, and K. Held, Towards ab initio calculations with the dynamical vertex approximation, J. Phys. Soc. Jpn. **87**, 041004 (2018).
[55] T. Ayral and O. Parcollet, Mott physics and spin fluctuations: A unified framework, Phys. Rev. B **92**, 115109 (2015).
[56] T. Ayral and O. Parcollet, Mott physics and spin fluctuations: A functional viewpoint, Phys. Rev. B **93**, 235124 (2016).
[57] T. Ayral, J. Vučičević, and O. Parcollet, Fierz Convergence Criterion: A Controlled Approach to Strongly Interacting Systems with Small Embedded Clusters, Phys. Rev. Lett. **119**, 166401 (2017).
[58] T. Ayral and O. Parcollet, Mott physics and collective modes: An atomic approximation of the four-particle irreducible functional, Phys. Rev. B **94**, 075159 (2016).
[59] E. A. Stepanov, V. Harkov, and A. I. Lichtenstein, Consistent partial bosonization of the extended Hubbard model, Phys. Rev. B **100**, 205115 (2019).

[60] E. A. Stepanov, Y. Nomura, A. I. Lichtenstein, and S. Biermann, Orbital Isotropy of Magnetic Fluctuations in Correlated Electron Materials Induced by Hund's Exchange Coupling, Phys. Rev. Lett. **127**, 207205 (2021).

[61] V. Harkov, M. Vandelli, S. Brener, A. I. Lichtenstein, and E. A. Stepanov, Impact of partially bosonized collective fluctuations on electronic degrees of freedom, Phys. Rev. B **103**, 245123 (2021).

[62] M. Vandelli, J. Kaufmann, M. El-Nabulsi, V. Harkov, A. I. Lichtenstein, and E. A. Stepanov, Multi-band D-TRILEX approach to materials with strong electronic correlations, SciPost Phys. **13**, 036 (2022).

[63] A. N. Rubtsov, M. I. Katsnelson, A. I. Lichtenstein, and A. Georges, Dual fermion approach to the two-dimensional Hubbard model: Antiferromagnetic fluctuations and fermi arcs, Phys. Rev. B **79**, 045133 (2009).

[64] H. Hafermann, G. Li, A. N. Rubtsov, M. I. Katsnelson, A. I. Lichtenstein, and H. Monien, Efficient Perturbation Theory for Quantum Lattice Models, Phys. Rev. Lett. **102**, 206401 (2009).

[65] S. Brener, E. A. Stepanov, A. N. Rubtsov, M. I. Katsnelson, and A. I. Lichtenstein, Dual fermion method as a prototype of generic reference-system approach for correlated fermions, Ann. Phys. (NY) **422**, 168310 (2020).

[66] A. Rubtsov, M. Katsnelson, and A. Lichtenstein, Dual boson approach to collective excitations in correlated fermionic systems, Ann. Phys. (NY) **327**, 1320 (2012).

[67] E. G. C. P. van Loon, A. I. Lichtenstein, M. I. Katsnelson, O. Parcollet, and H. Hafermann, Beyond extended dynamical mean-field theory: Dual boson approach to the two-dimensional extended Hubbard model, Phys. Rev. B **90**, 235135 (2014).

[68] E. A. Stepanov, E. G. C. P. van Loon, A. A. Katanin, A. I. Lichtenstein, M. I. Katsnelson, and A. N. Rubtsov, Self-consistent dual boson approach to single-particle and collective excitations in correlated systems, Phys. Rev. B **93**, 045107 (2016).

[69] E. A. Stepanov, A. Huber, E. G. C. P. van Loon, A. I. Lichtenstein, and M. I. Katsnelson, From local to nonlocal correlations: The dual boson perspective, Phys. Rev. B **94**, 205110 (2016).

[70] Y. M. Vilk and A.-M. S. Tremblay, Non-perturbative many-body approach to the Hubbard model and single-particle pseudogap, J. Phys. I **7**, 1309 (1997).

[71] H. Aizawa, K. Kuroki, and J.-i. Yamada, Enhancement of electron correlation due to the molecular dimerization in organic superconductors $\beta - (\mathrm{BDA} - \mathrm{TTP})_2 x (x = \mathrm{i}_3, \mathrm{sbf}_6)$, Phys. Rev. B **92**, 155108 (2015).

[72] S. Arya, P. V. Sriluckshmy, S. R. Hassan, and A.-M. S. Tremblay, Antiferromagnetism in the Hubbard model on the honeycomb lattice: A two-particle self-consistent study, Phys. Rev. B **92**, 045111 (2015).

[73] D. Ogura and K. Kuroki, Asymmetry of superconductivity in hole- and electron-doped cuprates: Explanation within two-particle self-consistent analysis for the three-band model, Phys. Rev. B **92**, 144511 (2015).

[74] K. Zantout, M. Altmeyer, S. Backes, and R. Valentí, Superconductivity in correlated bedt-ttf molecular conductors: Critical temperatures and gap symmetries, Phys. Rev. B **97**, 014530 (2018).

[75] T. Mertz, K. Zantout, and R. Valentí, Statistical analysis of the chern number in the interacting Haldane-Hubbard model, Phys. Rev. B **100**, 125111 (2019).

[76] J. M. Pizarro, S. Adler, K. Zantout, T. Mertz, P. Barone, R. Valentí, G. Sangiovanni, and T. O. Wehling, Deconfinement of mott localized electrons into topological and spin–orbit-coupled Dirac fermions, npj Quantum Mater. **5**, 79 (2020).

[77] H. Miyahara, R. Arita, and H. Ikeda, Development of a two-particle self-consistent method for multiorbital systems and its application to unconventional superconductors, Phys. Rev. B **87**, 045113 (2013).

[78] K. Zantout, S. Backes, and R. Valentí, Effect of Nonlocal Correlations on the Electronic Structure of LiFeAs, Phys. Rev. Lett. **123**, 256401 (2019).

[79] S. Bhattacharyya, K. Björnson, K. Zantout, D. Steffensen, L. Fanfarillo, A. Kreisel, R. Valentí, B. M. Andersen, and P. J. Hirschfeld, Nonlocal correlations in iron pnictides and chalcogenides, Phys. Rev. B **102**, 035109 (2020).

[80] N. Martin, C. Gauvin-Ndiaye, and A.-M. S. Tremblay, Nonlocal corrections to dynamical mean-field theory from the two-particle self-consistent method, Phys. Rev. B **107**, 075158 (2023).

[81] The Luttinger-Ward functional is a central functional in the Kadanoff-Baym formalism and defined as sum of all closed two-particle irreducible skeleton diagrams that can be constructed from the Green's function G and the Hubbard interaction U.

[82] Y. M. Vilk, L. Chen, and A.-M. S. Tremblay, Theory of spin and charge fluctuations in the Hubbard model, Phys. Rev. B **49**, 13267 (1994).

[83] J. P. F. LeBlanc and E. Gull, Equation of state of the fermionic two-dimensional Hubbard model, Phys. Rev. B **88**, 155108 (2013).

[84] J. P. F. LeBlanc, A. E. Antipov, F. Becca, I. W. Bulik, GarnetKin-Lic Chan, C.-M. Chung, Y. Deng, M. Ferrero, T. M. Henderson, C. A. Jiménez-Hoyos, E. Kozik, X.-W. Liu, A. J. Millis, N. V. Prokof'ev, M. Qin, G. E. Scuseria, H. Shi, B. V. Svistunov, L. F. Tocchio, I. S. Tupitsyn *et al.* (Simons Collaboration on the Many-Electron Problem), Solutions of the Two-Dimensional Hubbard Model: Benchmarks and Results from a Wide Range of Numerical Algorithms, Phys. Rev. X **5**, 041041 (2015).

[85] K. Zantout, The two-particle self-consistent approach and its application to real materials, Ph.D. thesis, Universitätsbibliothek Johann Christian Senckenberg (2021).

[86] Note that this ansatz breaks particle-hole symmetry, which is restored by averaging this expression with the particle-hole transformed expression as explained in Ref. [30]. In the following, we use the particle-hole symmetrized expression.

[87] The enforcement of crossing symmetry is, in principle, also in the pure multiorbital TPSC approach possible, but it was not performed in Refs. [30,78,85] as the symmetry $\Gamma^{\mathrm{sp},0}_{\alpha\alpha\beta\beta} = \Gamma^{\mathrm{sp},0}_{\alpha\beta\alpha\beta}$ is only valid in the longitudinal particle-hole channel, and this relation is used to argue for the symmetrization in Eq. (10). Keeping the symmetrization in the spin vertex whereas including the transversal particle-hole channel leads to an inconsistency in the argumentation.

[88] A. Gaenko, A. Antipov, G. Carcassi, T. Chen, X. Chen, Q. Dong, L. Gamper, J. Gukelberger, R. Igarashi, S. Iskakov, M.

Könz, J. LeBlanc, R. Levy, P. Ma, J. Paki, H. Shinaoka, S. Todo, M. Troyer, and E. Gull, Updated core libraries of the alps project, Comput. Phys. Commun. **213**, 235 (2017).

[89] H. Shinaoka, E. Gull, and P. Werner, Continuous-time hybridization expansion quantum impurity solver for multi-orbital systems with complex hybridizations, Comput. Phys. Commun. **215**, 128 (2017).

[90] A. Sushchyev and S. Wessel, Thermodynamics of the metal-insulator transition in the extended hubbard model from determinantal quantum monte carlo, Phys. Rev. B **106**, 155121 (2022).

[91] A.-M. Daré, L. Raymond, G. Albinet, and A.-M. S. Tremblay, Interaction-induced adiabatic cooling for antiferromagnetism in optical lattices, Phys. Rev. B **76**, 064402 (2007).

[92] C. Gauvin-Ndiaye, C. Lahaie, Y. Vilk, and A.-M. S. Tremblay (unpublished).

[93] M. Jarrell and J. Gubernatis, Bayesian inference and the analytic continuation of imaginary-time quantum monte carlo data, Phys. Rep. **269**, 133 (1996).

[94] R. Levy, J. LeBlanc, and E. Gull, Implementation of the maximum entropy method for analytic continuation, Comput. Phys. Commun. **215**, 149 (2017).

[95] G. Rohringer and A. Toschi, Impact of nonlocal correlations over different energy scales: A dynamical vertex approximation study, Phys. Rev. B **94**, 125144 (2016).

[96] J. Stobbe and G. Rohringer, Consistency of potential energy in the dynamical vertex approximation, Phys. Rev. B **106**, 205101 (2022).